Article

DNN-Based Physical-Layer Network Coding for Visible Light Communications

Xuesong Wang [1,2], Runxin Zhang [1,2], Xinyan Xie [1,2] and Lu Lu [1,2,*]

1   University of Chinese Academy of Sciences, Beijing 100049, China
2   Key Laboratory of Space Utilization, Technology and Engineering Center for Space Utilization,
     Chinese Academy of Sciences, Beijing 100094, China
*   Correspondence: lulu@csu.ac.cn

Abstract: The key difference between visible light communication (VLC) and radio frequency (RF) communication is the former's line-of-sight (LOS) transmission nature, and hence a relay node has to be adopted for VLC to extend its coverage. Physical-layer network coding (PNC) has the advantage of doubling the throughput of a two-way relay network (TWRN), where two end nodes exchange information via the help of a relay, compared with the conventional store-and-forward routing strategy. Although PNC has been studied for VLC in the literature, the state-of-the-art schemes are highly inefficient, requiring tight phase synchronization between the two end nodes, and hence difficult to realize. This paper proposes the application of a deep neural network (DNN) to a PNC VLC system, named DP-VLC, that enables misaligned phases and can deal with the light channel gains and noises in a satisfactory manner without introducing additional computation complexities. We implement DP-VLC using the universal software radio peripheral (USRP) software radio platform and a self-developed VLC optical front-end using commercial off-the-shelf (COTS) light-emitting diodes (LEDs) and photo-diodes (PDs). We find that irregular constellations generated by DP-PNC can be transmitted and recovered in a 1.5 m VLC link effectively. Experimental results show that our DP-PNC prototype performs better than conventional PNC VLC system when the signal-interference-to-noise ratio (SINR) of received optical signals is larger than 13.63 dB and can achieve a throughput of up to 77.38 Mbps in a 20 MHz channel under PNC scheme when the SINR is 22.86 dB. More importantly, we find that DP-VLC performs even better than fixed-constellation PNC system in the saturated SINR regime (e.g., 20–25 dB) where non-linear effects may happen compared with moderate SINR regimes (e.g., 10–20 dB), showing its adaptability to unpredictable impairments in optical links. Our first attempt at realizing DNN-based optical PNC in a TWRN has paved the way for future PNC-enhanced VLC systems.

Keywords: visible light communications; deep neural network; physical-layer network coding; orthogonal frequency division multiplexing

1. Introduction

Visible light communications (VLC) is considered to be the complement of traditional wireless communications in the 6th generation (6G) that can use light-emitting diodes (LEDs) as a light source to exchange high-speed data while meeting lighting needs. VLC has attracted significant interest recently for its cost efficiency, electromagnetic interference immunity, and high security, and has been studied under various scenarios, including multi-input-multi-output (MIMO)-based VLC using LED arrays [1], underwater VLC system [2], safety beamforming design [3], and non-orthogonal multiple access [4].

Since VLC systems are light-of-sight (LOS) systems, which means that users may have an effective communication range, a relay node can be used to expand the signal coverage of the system. Physical layer network coding (PNC) can be adopted under the scenario that two users in a VLC system who cannot communicate with each other because of non-LOS

are all under the relay's coverage, hence the system throughput can be doubled compared to the traditional point-to-point (Pt2Pt) architecture [5], by allowing signals sent by the users superimposed together at the relay node without information loss (Figure 1). There are notable works that studied PNC-based VLC systems. Hong et al. [5] demonstrated an adaptive bit-and-power-loading-based PNC VLC system that can allocate the bits to different subcarriers according to their estimated SNRs. Guan et al. [6] performed a PNC VLC system that needed a phase-aligning method to improve the performance, but the phase alignment is a strong condition that is hard to follow with different users.
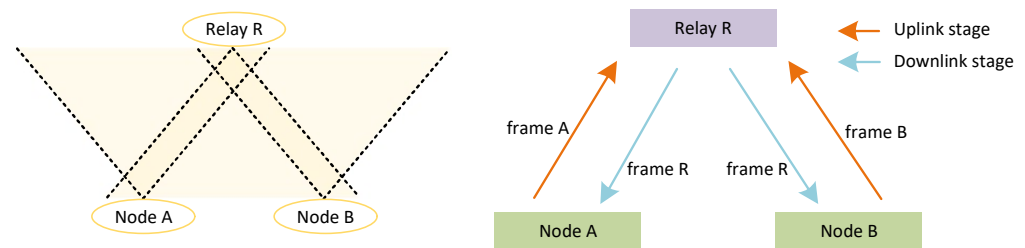

Figure 1. VLC system in TWRC under a PNC scheme.

Artificial intelligence (AI) and machine learning (ML) have become promising methods that activate the inspiration of enhancing the performance of VLC systems. Most of the previous works are focused on performing the network as a module of the system under different but specific scenarios [7–10]. There are previous works that show that a deep neural network (DNN) can simulate the whole communication system by enabling asynchronized constellations according to channel states and equalizing the received samples at the same time [11–14]. Although these works are mostly simulations and may not be suitable to implement the DNN-based VLC system, they give us the inspiration that misaligned phases as well as the light channel gains and noises can be dealt with together in a more intelligent way.

In this paper, we implement a prototype that merges the DNN with VLC that uses machine-generated misaligned constellations and is adaptive to the changeable channel states, while PNC is exploited to double the system's throughput. The pre-trained DNN model is detachable and can be inserted into hardware implementation to guarantee the adaption of phase misalignment and channel impairments together (see in Table 1). We follow the IEEE 802.11bb draft 2.0 and design the self-developed optical front-end pair that uses a radio frequency (RF) signal as input and converts the RF to an intermediate frequency (IF) to drive the LEDs to send optical signals. Experimental results show that our DP-PNC prototype can achieve a throughput of up to 38.69 Mbps per user under the PNC scheme when the SINR is around 22.86 dB and a total system throughput of 77.38 Mbps.

Table 1. Contribution comparison of VLC systems.

Topics	[5]	[6]	[7]	[8]	[9]	Our Work
Machine learning			✓	✓	✓	✓
Phase-misaligned constellations			✓			✓
Post equalization	✓		✓	✓		✓
PNC scheme	✓	✓				✓

2. System Model

In this section, we will first describe the PNC model and DNN-simulated architecture of the PNC system, show the generated constellations that will be used in the implementation of the DP-VLC system in later sections, and then describe the DP-VLC architecture that is performed in the experiments in Section 3.

2.1. DNN-Based PNC Design

Suppose there are two user nodes exchanging information with the help of the relay in a two-way relay network (TWRN) when both user nodes are under the relay's coverage but cannot communicate directly because of non-LOS. PNC can double the throughput by reducing transmission time slots from four to two under the half-duplex assumption under the scenario [15], as shown in Figure 1. First, both node A and node B transmit signals to the relay in the uplink stage simultaneously. In this way, the relay will receive the superimposed signal in the uplink stage

$$\boldsymbol{y}_R = \boldsymbol{h}_A \boldsymbol{x}_A + \boldsymbol{h}_B \boldsymbol{x}_B + \boldsymbol{w}, \tag{1}$$

where $\boldsymbol{y}_R = \{y_R^1, \cdots, y_R^N\}$, $\boldsymbol{x} = \{x^1, \cdots, x^N\}$, $\boldsymbol{h} = \{h^1, \cdots, h^N\}$, and $\boldsymbol{w} = \{w^1, \cdots, w^N\}$ are the signal received by relay R, the signal sent by node A or B, the channel coefficients, and the noise, respectively, and N is the length of received samples.

After the relay receives $\boldsymbol{y}_R$, it processes the signal into $\boldsymbol{x}_R$, which can be expressed as

$$\boldsymbol{x}_R = \mathcal{F}_R(\boldsymbol{y}_R), \tag{2}$$

and then broadcasts $\boldsymbol{x}_R$ to both users. Next in the downlink stage, user nodes receive $\boldsymbol{x}_R$ and exploit a local copy that has been sent before to recover the signal sent by the other node, which can be described as

$$\text{node A: } \boldsymbol{x}_B = \mathcal{F}_R(\boldsymbol{x}_R, \boldsymbol{x}_A); \text{ node B: } \boldsymbol{x}_A = \mathcal{F}_R(\boldsymbol{x}_R, \boldsymbol{x}_B). \tag{3}$$

In this paper, we follow the PNC mapping in the infinite field (PNCI) [15] to perform denoising at the relay and signal recovery at each node in the downlink. PNCI can be expressed as

$$\boldsymbol{x}_R = \mathcal{F}_R(\boldsymbol{y}_R | \boldsymbol{c}_A, \boldsymbol{c}_B, \boldsymbol{c}_R) = \left\{ \arg\max_{c_R = c_A + c_B} \left(\log \left(\exp \left(-\frac{|y_R - h_A c_A - h_B c_B|^2}{2\sigma^2} \right) \right) \right) \right\}, \tag{4}$$

where $c_A \in \boldsymbol{c}_A$, $c_B \in \boldsymbol{c}_B$ refer to the modulated constellation points under 2^k-QAM modulation type in node A and node B, $c_R \in \boldsymbol{c}_R = \{c_R \mid c_R = c_A + c_B\}$ means the standard receiving constellation at the relay node when $\boldsymbol{h} = 1$ and without noise, σ is the standard variance of noise. Equation (4) can be simplified as

$$\boldsymbol{x}_R = \mathcal{F}_R(\boldsymbol{y}_R | \boldsymbol{c}_A, \boldsymbol{c}_B, \boldsymbol{c}_R) = \left\{ c_R \; \middle| \; \arg\min_{c_R = c_A + c_B} \left(|y_R - h_A c_A - h_B c_B|^2 \right) \right\}, \tag{5}$$

which means to judge the Euclidean distance between received symbol y_R and relay's standard receiving constellation $c'_R \in \boldsymbol{c}'_R = \{c'_R \mid c'_R = h_A c_A + h_B c_B\}$, and find the c_R, which refers to the minimum distance, as the mapping target. In the downlink, after the relay's broadcasted signal $\boldsymbol{x}_R$ is received by both user nodes, similar processes are performed at node A and node B as

$$\text{node A: } \hat{x}_B = \mathcal{F}_A(\boldsymbol{x}_R, \boldsymbol{x}_A | \boldsymbol{c}_B) = \left\{ c_B \; \middle| \; \arg\min_{c_B} \left(|(x_R - x_A) - c_B|^2 \right) \right\},$$

$$\text{node B: } \hat{x}_A = \mathcal{F}_B(\boldsymbol{x}_R, \boldsymbol{x}_B | \boldsymbol{c}_A) = \left\{ c_A \; \middle| \; \arg\min_{c_A} \left(|(x_R - x_B) - c_A|^2 \right) \right\}, \tag{6}$$

to recover the signal sent by the other node.

Note that by using Equation (6), a perfect downlink is assumed, which means no channel coefficient is considered in the downlink and the signal from relay R is directly sent to nodes A and B without impairment. This is a common premise since the procession

of downlink in PNC is the same with Pt2Pt [15]. So we mainly focus on the distortions in uplink and treat the downlink as a perfect channel without loss of generality.

In this way, PNC uses two time slots to finish the information exchange between two user nodes. As a comparison, the traditional half-duplex system cannot make use of signal collision, hence the information exchange uses four time slots that are presented as: time slot 1, node A sends x_A to relay R; time slot 2, relay R sends x_A to node B; time slot 3, node B sends x_B to relay R; time slot 4, relay R sends x_B to node A. PNC reduces two time slots comparing to the traditional scenario, hence the throughput is doubled by using an equal length of time.

To simulate the PNC system using a DNN, we build the DNN architecture to follow the signal flow in the PNC system, as shown in Figure 2. A DNN-based PNC model can also be divided into the uplink stage and downlink stage. In the uplink stage, there are two encoders that modulate the input source bits $s_A = \{s_A^1, \cdots, s_A^N\}$ and $s_B = \{s_B^1, \cdots, s_B^N\}$ into ready-to-transmit signals x_A and x_B, respectively. To be specific, source bits $s_A^i \in \{0, 1\}^k$ are embedded into one-hot-vector v_A^i with length of each v equaling to 2^k; so as the node B. For example, if $s_A = \{10\}$ when $k = 2$ ("10" is 3 in decimal), then the third element in v_A is set to be 1 and others to be 0. v is then sent into multiple layer perceptron (MLP) as input. MLP is established by several linear layers and the Leaky ReLU layer as the activation function in the output layer. Signals are power-normalized before being transmitted to the relay. Relay performs $\mathbb{R} \to \mathbb{R}$ mapping to convert the received signal y_R into x_R. Next, in the downlink stage, the relay broadcast x_R to both decoders, and the decoder A and decoder B retrieve the estimation of v_B and v_A, refer as $\hat{v}_B$ and $\hat{v}_A$, utilizing x_R and a copy of previous-sent signals x_A and x_B. $\hat{v}_A$ and $\hat{v}_B$ are then de-embedded by finding the maximum number's index and transferring the (decimal) index into binary bits whose length is k. Note that a pair of encoder and decoder refers to the modulation module and demodulation module of the same node. The behavior of encoders, relays, and decoders can be adaptive based on the back-propagation of machine learning in the training stage according to the channel state.
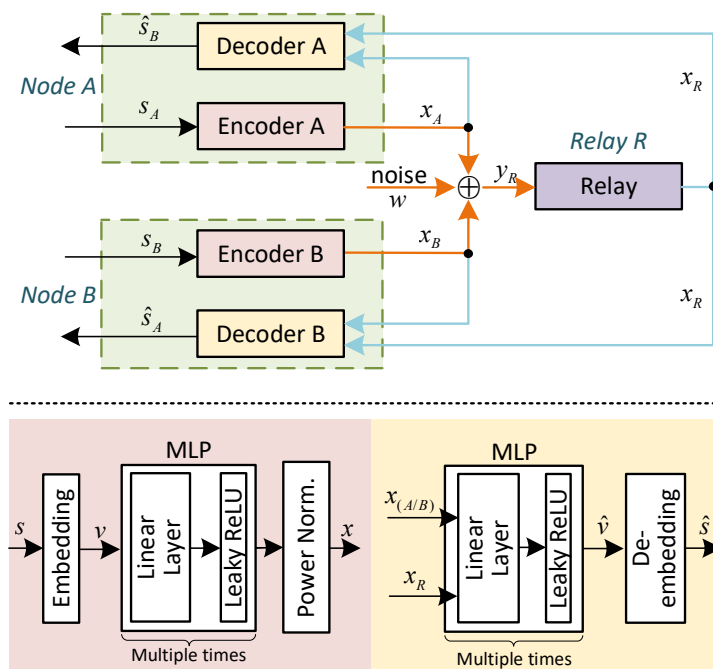

Figure 2. DNN-based PNC scheme. A pair of encoder and decoder refers to the modulation module and demodulation module of the same node. We use the same color as in Figure 1 to show the uplink and downlink stages.

To further explain the function of the DNN-based PNC network with the signal flow that is mentioned above, let $\mathcal{E}()$, $\mathcal{R}()$, and $\mathcal{D}()$ refer to the function of encoders, relays, and

decoders, respectively, then the aim of the training is to minimize the cross-entropy loss function that can be described as

$$\begin{aligned}
\mathcal{L}_{loss} &= -\sum_N s_A \log(\hat{s}_A) - \sum_N s_B \log(\hat{s}_B) \\
&= -\sum_N s_A \log(\mathcal{D}(x_R - x_B)) - \sum_N s_B \log(\mathcal{D}(x_R - x_A)) \\
&= -\sum_N s_A \log(\mathcal{D}(\mathcal{R}(y_R) - \mathcal{E}(s_B))) - \sum_N s_B \log(\mathcal{D}(\mathcal{R}(y_R) - \mathcal{E}(s_A))).
\end{aligned} \tag{7}$$

Unlike conventional communication systems, the bit/block error rate may not be an appropriate performance metric for DNN-based communication systems. Generalized mutual information (GMI) is probably the appropriate metric that should be maximized since DNNs behave differently than usual modulators or demodulators [13]. The goal of training is to minimize the cross-entropy loss between input and output estimates instead of using conventional measures like soft-decision forward error correction, and it directly maximizes the achievable sum rate in terms of GMI. The normalized GMI in data communication is expressed as [13]

$$\text{GMI} = 1 - \mathbb{E}_{b,L}\left[\log_2\left(1 + \exp(-(-1)^b)L\right)\right], \tag{8}$$

where $L = \Pr(b = 0)/\Pr(b = 1)$ is the log-likelihood ratio (LLR) corresponding to the information bit b. The achievable sum rate can be expressed as

$$2k(1 - \mathbb{E}[\mathcal{L}_{loss}])(\text{bps/Hz}), \tag{9}$$

where 2 means two user nodes and k refers to the modulation order parameter. In this paper, we focus on achievable sum rate and verify that DP-VLC has good performance in achievable sum rate in later experiments.

DNN-based PNC systems do not have regular constellation patterns, and the constellations generated by encoders are always misaligned, as shown in Figure 3. Here are some explanations. First, the input dimension of DNN determines the upper limit of the number of constellations. To specify, if encoder A maps a group of source bits $s_A \in \{0,1\}^k$ into one-hot vector set $v_A = \{v^1, \cdots, v^N\}$ with the length of each v equaling to 2^k, then the dimension of inputs to the multi-layer perceptron (MLP) of encoder A is 2^k and there will be up to 2^k groups of constellations (called 2^k-QAM) when analyzing the output x_A; and the same with encoder B. Next, although the middle layers of the MLP provide efficient (but not too large to drop the processing speed or to lead to overfitting) dimensions to the signal to be expanded and processed, the behaviors of the middle layers are unknown during the training. Moreover, the initial parameters and channel states can also affect the output constellation patterns. As a result, constellations generated by different encoders may not have the same number of constellation points compared to each other and compared to conventional constellation patterns, and may converge into different locations in different training (Figure 3). To conclude, the constellations generated by DNN are misaligned between both encoders.

When we focus on a symbol of the received signal at the relay node, we can further express Equation (1) as

$$y_R = |h_B|e^{\phi_B}\left(\frac{|h_A|}{|h_B|}e^{(\phi_A - \phi_B)}x_A + x_B + w\right), \tag{10}$$

where $h_A = |h_A|e^{\phi_A}$, $h_B = |h_B|e^{\phi_B}$, and $\phi = \phi_A - \phi_B$ is the phase asynchrony between both signals in the uplink. For a fixed-constellation-based PNC system, asynchrony between the two signals in the uplink is the most important reason that causes the throughput damage [16]. Phase aligning, or say phase synchrony, can improve the performance [6], but phase alignment is hard to achieve in real implementation since the two signals are

through different channels. By using a DNN, we let encoders add the asynchrony before the transmission, while this "asynchrony" is fine-tuned between two user nodes by training the DNN (Figure 3). So the system will not have to ensure the synchrony between two signals and the system throughput can be improved in the usual way.
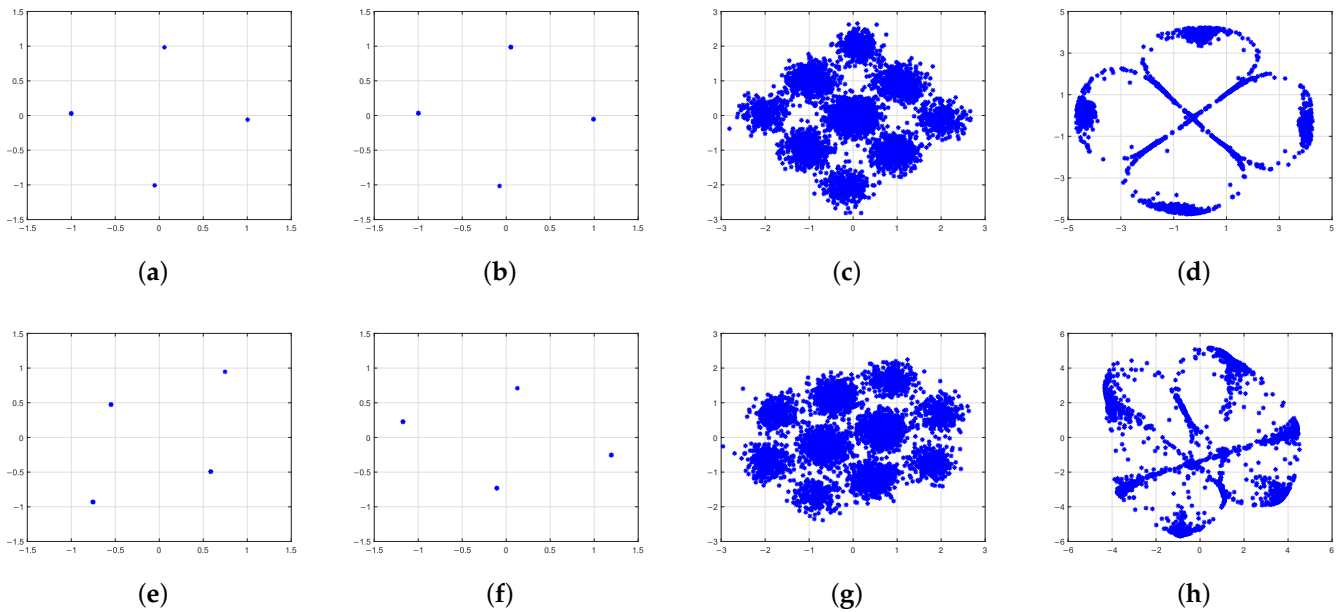

Figure 3. Constellations generated after the training processes. Each row of subfigures shows a group of representative training outputs of our DNN-based PNC model during different training. (**a**,**e**) encoder A output; (**b**,**f**) encoder B output; (**c**,**g**) relay input; (**d**,**h**) relay output.

Details of the network structure are as follows. Only fully connected layers are used in MLPs in encoders, relays, and decoders. Leaky ReLU is used as the activation function in the output layer of encoders and relays. Note that our network has a simple architecture with low computation complexity and is easy to implement. There are three middle layers in the encoders and decoders at user nodes and four middle layers at the relay node, and each middle layer contains 128 dimensions. The structure of the DNN used in the training stage is optimized by setting and repeatedly testing different numbers of inner layers and different numbers of dimensions in each layer of encoders, relays, and decoders. We find a balance between computational complexity and the achievable sum rate that our DNN model can get to make sure that the combination with the VLC channel performs well in Section 3. Compared to the DNN-based PNC model used in [13], our model has deeper layers but fewer training parameters. Our model has a total of 189,966 training parameters, while the model in [13] has more than 5×10^6 parameters.

We use Adam optimizer

$$\mathcal{A} = \begin{cases} \hat{m}_t = \frac{m_t}{1-\beta_1^t}, \\ \hat{v}_t = \frac{v_t}{1-\beta_2^t}, \\ \theta_{t+1} = \theta_t - \frac{\eta}{\sqrt{\hat{v}_t}+\epsilon} \hat{m}_t \end{cases} \tag{11}$$

as optimize function where $\hat{m}_t$ and $\hat{v}_t$ are the first-order and second-order moment estimation of gradient, $\beta_1 = 0.9$, $\beta_2 = 0.99$, θ is the parameter set of the training network, and ϵ is a small positive number that makes sure the denominator is not zero. Adam optimizer is a momentum-based algorithm that exploits the history of gradients. It combines the advantage of AdaGrad and RMSProp and is often used in DNN training [17]. Adam is easy to fine-tune, can get good results quickly, and can deal with large training data efficiently. It

is also widely used in other DNN-based communication systems [12,13]. The cross-entropy loss function (Equation (7)) is performed as the training target.

During the training, we use a variable learning rate that is equal to 0.0002 at the beginning of training and is multiplied by 0.8 every 20 epochs. The network will be pre-trained under additive white Gaussian noise (AWGN) channel to focus on the ability of constellation generation at encoders, while the post-equalization ability of DNN can be ensured by analyzing the outputs of each module. Signal damages in the VLC channel such as shot noise, thermal noise, and the environment light interference will be jointly processed by both DNN and OFDM framework in the implementation in Section 2.2.

2.2. DP-VLC System

As mentioned above, the DNN-based PNC model is separated into encoders, relays, and decoders, referring to the modulator, relay, and demodulator, respectively, so these DNN modules can be taken out as part of the whole DP-VLC system. Since the procession of downlink in PNC that relays broadcasts signal to the user nodes is the same with Pt2Pt, here we mainly focus on the distortions in uplink and treat the downlink as a perfect channel without loss of generality. These two conditions are the premises of our experiments later.

The setup of our DP-VLC using PNC is depicted in Figure 4a. Node A, node B, and relay R are framed with different kinds of colors, and the orange lines present the signal transmission in the uplink stage. A dash-framed "optical link" represents the indoor VLC channel with optical integrated front-ends involved. The front-ends are self-developed and accept 2.43 GHz RF signals as input. At node A and node B, source bits are fed into the well-pre-trained encoder modules to generate misaligned constellations. The 64-point IFFT and up-conversion modules are performed to create real-time RF signals. Optical front ends include several sub-modules that are shown in Figure 4b–e. Mixers using a local oscillator can convert the signal to an appropriate IF range that falls into the LEDs' linear range at optical front-end A/B and can convert IF range signals into RF that meets the down conversion component's need at the relay. At front-end A/B, electro-optical (EO) components use an amplifier and a pre-equalization circuit to convert voltage signal to a current signal that drives LED to send signals. At front-end R, the optical-electro (OE) component has several sub-modules: a PIN photo-diode is selected and a trans-impedance amplifier (TIA) is used to convert the current signal into a voltage signal; power amplifier (PA) is performed to amplify the signal. The pre-equalization (in EO) and post-equalization (in OE) are used to compensate for the non-linearity of the LED. We designed our EO and OE modules based on IEEE 802.11bb. We have tested our EO and OE hardware, and the optical bandwidth is 200 MHz which is large enough for the 20 MHz DNN-PNC system implementation. After the relay mixes the RF signal into the baseband signal using the down conversion module, an OFDM receiver is used to recover the superimposed signal. Note here that the superimposed signal is different from "$\boldsymbol{y}_R$" in Section 2.1 because extra processes are performed after receiving the signals in the air. However, we keep the same notation since they are both considered to be the input to the DNN-relay module. The relay performs $\mathcal{R}(\boldsymbol{y}_R)$ to further denoise and post-equalizing. The "DNN-decoder" blocks are followed to depict that signals from the DNN-relay module are fed into the DNN-decoder blocks directly with the perfect downlink assumption, and the bit-error-rate (BER) calculator block is used to calculate BER by exploiting the outputs from decoders and the source bits from node A and B as local copies.

The signals in the uplink stage from both nodes may not be well aligned in the time domain in the real implementation. To deal with the two uplink VLC signals being asynchronous, we inherit the OFDM frame format as described in chapter 5 of [15], with a well-designed OFDM preamble that is suitable for a PNC system with an 8000-sample-long payload. In the payload of each OFDM frame, 48 data samples of every 64 data samples are loaded as available subcarriers with a 16-sample-long cyclic prefix (CP) loaded ahead. The OFDM receiver at the relay node that contains sub-blocks to deal with carrier frequency offset (CFO) and channel estimation under the PNC scheme allows the signals to

be misaligned within 16 samples. Details of the design of OFDM frames are not the core of this manuscript and are not detailed here.
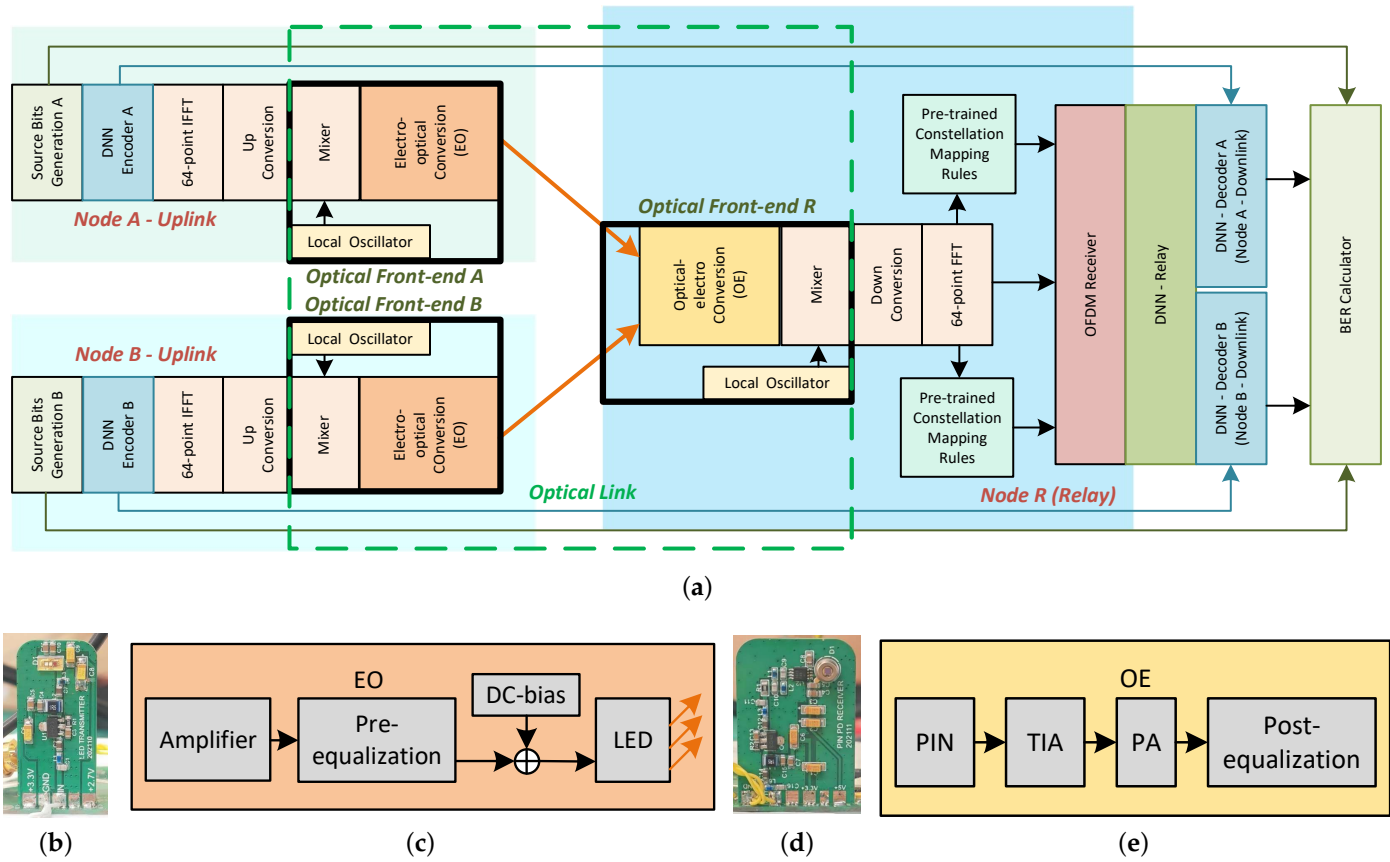

Figure 4. DP-VLC system design. (**a**) The whole system of DP-VLC; (**b**) electro-optical conversion component and (**c**) its circuit diagram; (**d**) optical-electro conversion component and (**e**) its circuit diagram.

Note that a pre-trained constellation mapping rules module is needed and is important to the system's performance. It increases the system's complexity compared to the conventional PNC-VLC system that does not have to consider mapping rules [18]. The reasons are described as follows. The constellation mapping rules are different from traditional patterns and the behaviors of all modules in DNN are implicit. One can only ensure reliability by analyzing the output constellations and error rates of received signals. Moreover, mapping rules of modulation or demodulation are separated and irrelative because a user node is divided into an encoder–decoder pair; the relay module does not know anything about the constellations by analyzing the input and output of the relay; the relay can only denoise and cluster constellations by analyzing Figure 3 and prior knowledge does not need to be involved. However, when signals arrive at the relay node in the implementation, the relay has to deal with channel impairments that are mentioned above at first. Hence, prior knowledge $c'_R \in \boldsymbol{c}'_R = \{c'_R \mid c'_R = h_A c_A + h_B c_B\}$ has to be known to the relay node when considering the real VLC channel to help to deal with channel damages (Equation (4)). For these reasons, the mapping rules, which are obtained by clustering the encoders' output constellations into (up to) 2^k groups and calculating the centers (noted as $\boldsymbol{c}_A$ and $\boldsymbol{c}_B$ in Equation (4)), are together sent with data from both nodes (encoders) to the relay, and relay extracts the prior knowledge before recovers the data. The reason for clustering is that, when encoders map $\boldsymbol{v}$ to $\boldsymbol{x}_A$ or $\boldsymbol{x}_B$, the constellations actually gather into 2^k groups and look like some type of QAM visually, with a number of points in each group (Figure 3). Traversing all the distances $|y - h_A x_A^i - h_B x_B^j|$ in Equation (5) is not a proper method for

the relay node. So we use the clusters of constellations to represent all the constellations generated by encoders, which means $i, j \leq 2^k$. Some accuracy may be lost but the calculation is simplified in this way. Note that prior knowledge is also through the VLC channel and suffers impairment, which means a chain reaction, so the training state affects the constellations generated by encoders and the clusters of constellations, and further affects the prior knowledge recovery and data recovery at the relay node.

3. Experiments, Results, and Discussions

In the experiments, we set up $k = 2$ to show the system's performance. To illustrate the system performance of DP-VLC, we implement three other VLC systems that also use PNCI as comparisons with our DP-VLC and prepare 1000 OFDM frames to transmit under each scenario:

- fixed-constellation PNC VLC system (named PNC-VLC), which uses conventional constellation patterns to modulate and demodulate signals by replacing the DNN module with traditional QAM modulator and demodulator, and other modules remain the same;
- DNN Pt2Pt-VLC system (named D-Pt2Pt-VLC) that uses DNN-generated constellations, but only one of the user nodes transmits the signal. To achieve this scenario, the optical front-end B is shut down without generality so that signals of node B are neglected;
- fixed-constellation Pt2Pt-VLC system (named Pt2Pt-VLC) that uses conventional constellations under Pt2Pt-VLC scenario.

There are two main stages in the experiments with the DNN: (1) the training stage that can get the well-pre-trained modules mentioned above, and (2) the communication stage that embeds these modules with other modules that belong to visible light communication (VLC) system to deal with signals in the air. In the first stage, to be specific, DNN modules are trained under SNR = 9 dB when $k = 2$ to ensure that DNN modules can generate constellations and deal with channel damages reasonably [13], hence the system could perform well in the recovery chain reaction that is mentioned above. In the second stage, pre-trained modules are separated and embedded with other modules that belong to OFDM as well as optical hardware pieces to handle signals in the VLC system.

Figure 5 shows the hardware that is used in the implementation of DP-VLC. There are two front ends instead of three, and the left optical front end is used as node A or node B while the right front end is used as the relay node. Frame misalignment within 16 samples is performed manually and randomly before putting the superimposed signal into the OFDM receiver. Here are some reasons to explain. The first reason is that our optical-electro (OE) component at the relay node does not have a large angle. To achieve the PNC VLC implementation, the current OE at the relay node needs a larger angle, but a larger angle leads to difficulty in adjusting SINR. The second reason is that in our two-front-end PNC VLC system, we emulated the superimposed signal at the relay node by transmitting signals from user nodes to relay one by one and added them manually by introducing a delay between two signals purposely. This procedure was also used in [19] and is equivalent to the signal's superimposing at the relay. We will leave the real-time three-node PNC VLC implementation with a larger angle OE to our future work.

In Figure 5, we use USRP-2974 as an upconverter at nodes A and B to mix the signal to 2.43 GHz that acts as radio frequency (RF) input to the front ends, and change the transmitting power by setting transmitter gain using GNU Radio (GNU Radio is a free and open-source software development toolkit that provides signal processing blocks to implement software radios; reference link: https://www.gnuradio.org accessed on 16 December 2022); USRP is also used as down-converter at the relay. The transmitter gain range of USRP-2974 is from 0 dB to 31.5 dB, and we choose seven values that are from 0 dB and stepped by 5 dB. The receiving signal-interference-to-noise ratio (SINR) is synchronously changed by setting the transmitter gain, and we calculate the received SINRs of optical signals at the optical front end. Note that it is the SINR, not SNR, that is

to be considered at the receiver of the relay because there is shot noise and thermal noise around, and the environment has visible light interference. We choose the center frequency of the local oscillator to be 2.43 GHz. Limited by the processing speed of USRP, we set the signal bandwidth to 20 MHz. Signals from node A and node B are transmitted to the relay node separately and are added after sampling the signals. In this way, oscillator asynchrony is avoided and we can further focus on the signal processing ability of our DP-VLC system without loss of generality. The zoomed subfigure in Figure 5 shows the real-time time-domain waveform and frequency spectrum of received optical signals.
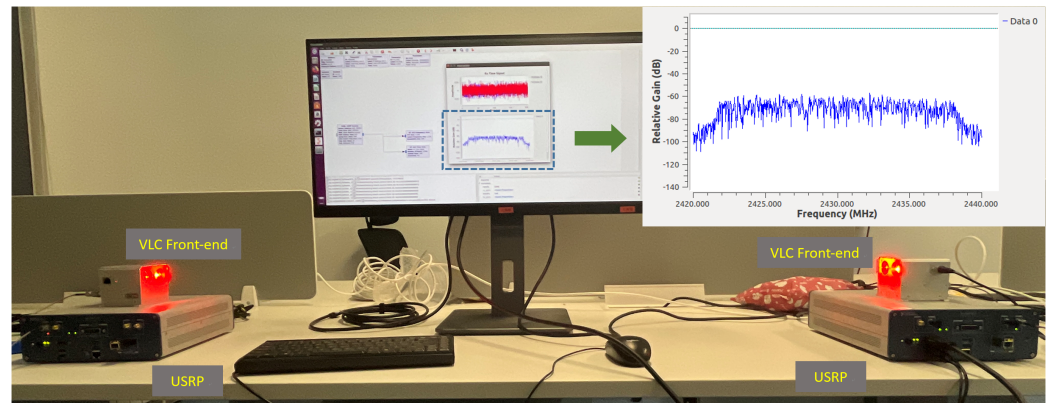

Figure 5. Hardware implementation used in our prototype of DP-VLC. The distance between the two optical front ends is 1.5 m. Personal computers used for training and signal processing are not shown here.

Figure 6 shows the experimental results of our DP-VLC system with a comparison of the other three implementations listed above. The blue lines and the green lines refer to VLC with PNC and VLC with Pt2Pt, respectively, while the solid lines and the dashed lines refer to implementation with DNN and without DNN, respectively. The orange bars represent the received SINR of optical signals at the relay's front end. Note that in a PNC system, the maximum sum rate is doubled compared to the Pt2Pt system under the same modulation type, so the maximum sum rate that a PNC system can achieve is 4 bps/Hz when $k = 2$. We can see that when the SINR is low, DP-VLC performs inferior to PNC-VLC by less than 0.25 bps/Hz, but when transmitter gain is larger than 10 dB, which leads to an SINR larger than 13.63 dB, DP-VLC runs better than PNC-VLC. When the SINR is 22.86 dB, both DP-VLC and PNC-VLC achieve the best performance of 3.869 bps/Hz and 3.849 bps/Hz based on our results. Since the sample rate that we use in the implementation is 20 MHz, the DP-VLC's system throughput is $20 \times 3.869 = 77.38$ Mbps, with average throughput 38.69 Mbps for each user node. Considering the Pt2Pt VLC scenarios, both implementations achieve a fully achievable sum rate of 2 bps/Hz when transmitter gain is larger than 15 dB, which means a total throughput of 40 Mbps. To conclude, our DP-VLC with misaligned constellations performs better than PNC-VLC when the SINR is higher than 13.63 dB and can achieve almost double throughput compared to Pt2Pt-VLC and D-Pt2Pt-VLC when the SINR is 22.86 dB based on our experiments.

We find that the DP-VLC performs inferior to PNC-VLC and D-Pt2Pt-VLC performs inferior to Pt2Pt-VLC when the SINR is low. Here we explain the reasons. The encoders, relay, and decoders are all made of a DNN that includes several inner layers. With these inner layers, signals can be considered as going through multiple coding or decoding step implicitly [13]. We have expert knowledge that signals with coding are likely to behave inferior to that without coding when the SNR is low, but have better performance when the SNR is high [16]. Our results indicate this expert knowledge by analyzing the curves under a low SINR in Figure 6, which verifies our results as being reliable.

Note that when the transmitter gain is larger than 20 dB, the SINR of received optical signals increases slower than before, and the system throughput of both PNC schemes

also increases slower and is even inferior when the transmitter gain is 30 dB. The reason can be explained as follows. When the SNR of the RF signal is large, restrictions on the circuit of optical hardware cannot be neglected, for example, mixers have input power limitations, power amplifiers have maximum output power limitations, and LEDs have modulation depth limitations, and these factors can lead to the signals' distortion. It can also be seen intuitively from the orange bars in Figure 6 that the received SINR no longer increases linearly when the transmitter gain is larger than 20 dB. Here, the mixer is the first to enter the non-linear region, and the throughput starts to slow down correspondingly. Considering the fact that constellations under the PNC scheme are more complex than the Pt2Pt scheme when transmitter gain is 30 dB, the distortion of the signal leads to system damage and causes a decrease in system throughput. However, we found that even if the hardware device enters the non-linear region, the DP-VLC system still operates better than PNC-VLC, showing its automatic adaptability to unpredictable impairments in optical wireless communications.
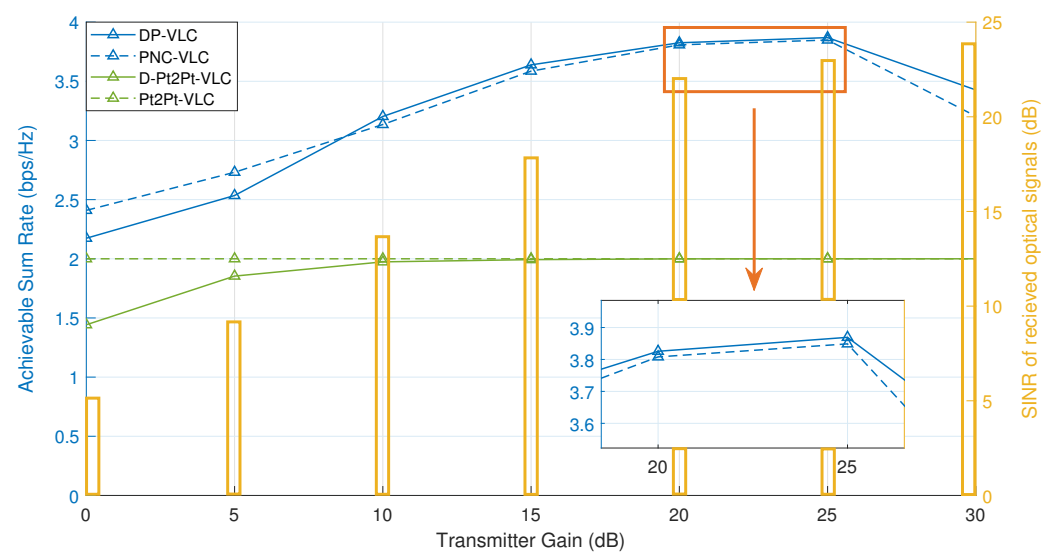

Figure 6. System performance of DP-VLC when $k = 2$ with comparison of PNC-VLC, D-Pt2Pt-VLC, and Pt2Pt-VLC under different transmitter gains.

Here we give another view of the systems' performance by analyzing the receiving frames of DP-VLC. Note that each OFDM frame from node A or node B is made of 9600 source bits, which means the minimum package error rate is 1.0417×10^{-4}. Figure 7 shows the histogram of a package error rate of OFDM frames in DP-VLC systems under SINRs between 13.63 dB and 23.8 dB, by setting transmitter gain from 10 dB to 30 dB in the step of 5 dB. Bars between 0 and 1×10^{-4} show that the package error rate is zero. We can see that when the SINR is lower than 21.97 dB, bars tend to gather to the left of each subfigure, which means the system has better performance when the SINR is higher. When the SINR is 22.86 dB, bars tend to gather in the middle of the subfigure compared to the left three subfigures. It is clear that the number of low-error-rate packages under an SINR equaling 22.86 dB is more than that under an SINR equaling 21.97 dB. It might indicate the damages caused by non-linear effects. When comparing the fourth and fifth subfigures in Figure 7, such an effect is more obvious that bars are going to gather on the right side. We further find that packages with high error rates pull up the average bit error rate, hence the achievable sum rate decreases, so the DP-VLC only achieves 1.93 times the throughput of the Pt2Pt-based VLC system. In the future, we could involve channel coding into the system, or drop the frames with high package error rates.
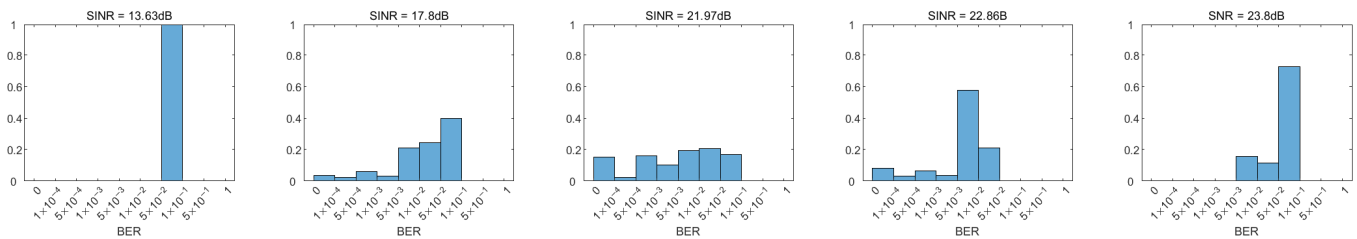
Figure 7. Histograms of a package error rate of DP-VLC systems.

4. Conclusions

Physical-layer network coding (PNC) has been studied for VLC recently and can double the system's throughput compared to a point-to-point (Pt2Pt) system, but the state-of-the-art literature of PNC VLC requires tight phase synchronization between the two end nodes, which is difficult to realize in the implementation. Since the DNN is demonstrated to generate misaligned constellations and perform post-equalization at the same time, in this paper, we expand the design into VLC systems and make suitable changes to be adaptive. Our prototype, called DP-VLC, merges the pre-trained detachable DNN model that can be separated as important components with the hardware pieces, including USRP and self-developed optical front end, to process the misaligned constellations and channel impairments together. DP-VLC uses PNC to double the throughput compared to Pt2Pt systems and can reach this doubled throughput in the usual way by allowing phase-misaligned constellations generated by DNN. Furthermore, we follow the IEEE 802.11bb to design the system implementation and perform experiments. The results show that our system can generate and transmit non-type constellations and recover signals effectively at the receiver, with a system throughput of up to 38.69 Mbps per user, and a total throughput of 77.38 Mbps, when the SINR is 22.86 dB. It is our first attempt in realizing DNN-based optical PNC in a TWRN system, and we can further optimize DP-PNC so as to increase the system throughput by adopting higher-order modulation and using a wider optical bandwidth in the near future.

Author Contributions: System model, simulation, and experimentation, X.W.; hardware implementation, R.Z. and X.X.; results discussion, X.W. and R.Z.; writing—original draft preparation, X.W.; writing—review and editing, R.Z., X.X. and L.L.; funding acquisition, L.L. All authors have read and agreed to the published version of the manuscript.

Institutional Review Board Statement: Not applicable.

Informed Consent Statement: Not applicable.

Data Availability Statement: Data are available upon reasonable request by the corresponding author.

Conflicts of Interest: The authors declare no conflict of interest.

References

1. Dixit, V.; Kumar, A. Error analysis of L-PPM modulated MIMO based multi-user NOMA-VLC system with perfect and imperfect SIC. *Appl. Opt.* **2022**, *61*, 858–867. [CrossRef] [PubMed]
2. Geldard, C.; Thompson, J.; Popoola, W.O. A study of non-orthogonal multiple access in underwater visible light communication systems. In Proceedings of the 2018 IEEE 87th Vehicular Technology Conference (VTC Spring), Porto, Portugal, 3–6 June 2018; pp. 1–6.
3. Du, C.; Zhang, F.; Ma, S.; Tang, Y.; Li, H.; Wang, H.; Li, S. Secure transmission for downlink NOMA visible light communication networks. *IEEE Access* **2019**, *7*, 65332–65341. [CrossRef]
4. Lin, B.; Tang, X.; Ghassemlooy, Z. A power domain sparse code multiple access scheme for visible light communications. *IEEE Wirel. Commun. Lett.* **2019**, *9*, 61–64. [CrossRef]
5. Hong, Y.; Chen, L.K.; Zhao, J. Channel-aware adaptive physical-layer network coding over relay-assisted OFDM-VLC networks. *J. Light. Technol.* **2019**, *38*, 1168–1177. [CrossRef]

6.   Guan, X.; Yang, Q.; Wang, T.; Chan, C.C.K. Phase-aligned physical-layer network coding in visible light communications. *IEEE Photonics J.* **2019**, *11*, 1–9. [CrossRef]

7.   Lu, X.; Zhao, M.; Qiao, L.; Chi, N. Non-linear compensation of multi-CAP VLC system employing pre-distortion base on clustering of machine learning. In *Optical Fiber Communication Conference*; Optical Society of America: San Diego, CA, USA, 2018; p. M2K-1.

8.   Lu, X.; Lu, C.; Yu, W.; Qiao, L.; Liang, S.; Lau, A.P.T.; Chi, N. Memory-controlled deep LSTM neural network post-equalizer used in high-speed PAM VLC system. *Opt. Express* **2019**, *27*, 7822–7833. [CrossRef] [PubMed]

9.   Zhu, Y.; Gong, C.; Luo, J.; Jin, M.; Jin, X.; Xu, Z. Indoor Non-Line of Sight Visible Light Communication with a Bi-LSTM Neural Network. In Proceedings of the 2020 IEEE International Conference on Communications Workshops (ICC Workshops), Dublin, Ireland, 7–11 June 2020; pp. 1–6. [CrossRef]

10.   Zou, C.; Yang, F. Dimming-Aware Deep Learning Approach for OOK-Based Visible Light Communication. *J. Light. Technol.* **2020**, *38*, 5733–5742. [CrossRef]

11.   O'shea, T.; Hoydis, J. An introduction to deep learning for the physical layer. *IEEE Trans. Cogn. Commun. Netw.* **2017**, *3*, 563–575. [CrossRef]

12.   Erpek, T.; O'Shea, T.J.; Sagduyu, Y.E.; Shi, Y.; Clancy, T.C. Deep learning for wireless communications. In *Development and Analysis of Deep Learning Architectures*; Springer: Berlin/Heidelberg, Germany, 2020; pp. 223–266.

13.   Matsumine, T.; Koike-Akino, T.; Wang, Y. Deep learning-based constellation optimization for physical network coding in two-way relay networks. In Proceedings of the ICC 2019—2019 IEEE International Conference on Communications (ICC), Shanghai, China, 20–24 May 2019; pp. 1–6.

14.   Park, J.; Ji, D.J.; Cho, D.H. High-Order Modulation Based on Deep Neural Network for Physical-Layer Network Coding. *IEEE Wirel. Commun. Lett.* **2021**, *10*, 1173–1177. [CrossRef]

15.   Liew, S.C.; Lu, L.; Zhang, S. A primer on physical-layer network coding. *Synth. Lect. Commun. Netw.* **2015**, *8*, 1–218.

16.   Lu, L.; Liew, S.C. Asynchronous physical-layer network coding. *IEEE Trans. Wirel. Commun.* **2011**, *11*, 819–831. [CrossRef]

17.   Kingma, D.P.; Ba, J. Adam: A method for stochastic optimization. *arXiv* **2014**, arXiv:1412.6980.

18.   Lu, L.; Wang, T.; Liew, S.C.; Zhang, S. Implementation of physical-layer network coding. *Phys. Commun.* **2013**, *6*, 74–87. [CrossRef]

19.   Marcum, A.C.; Krogmeier, J.V.; Love, D.J.; Sprintson, A. Analysis and implementation of asynchronous physical layer network coding. *IEEE Trans. Wirel. Commun.* **2015**, *14*, 6595–6607. [CrossRef]